Hindawi
Shock and Vibration
Volume 2020, Article ID 8876187, 15 pages
https://doi.org/10.1155/2020/8876187

Research Article

Tool Wear Assessment Approach Based on the Neighborhood Rough Set Model and Nearest Neighbor Model

Ren Sheng and Xiaoran Zhu

School of Mechanical Engineering, Yellow River Conservancy Technical Institute, Kaifeng, Henan, China

Correspondence should be addressed to Xiaoran Zhu; xiaoran.zhu@foxmail.com

Received 15 July 2020; Revised 11 November 2020; Accepted 5 December 2020; Published 17 December 2020

Academic Editor: Li Qing

In order to assess the degree of wear of tool for milling process quantitatively, a new assessment approach is proposed. Firstly, making full use of the neighbor information, two sensitive features are selected by using the neighborhood rough set model, and then, boundary curves are established by using the nearest neighbor model with noncounter data in two dimension spaces. Secondly, the intersection area or expanding area is used to describe the difference between two boundary models because the intersection area or expanding area can consider the effect of distance and angle simultaneously in two dimension spaces. Thirdly, after determining a baseline state, a new quantitative assessment indicator (QAI) can be calculated based on the intersection area or expanding area. The QAI can directly measure the difference between the model of baseline state and the model of unknown state and indirectly measure the degree of wear of tool. Finally, the effectiveness of the assessment approach is proven by using the Milling Dataset which was provided by the NASA Ames Research Center.

1. Introduction

In order to guarantee the quality and productivity of the machining process, tool condition monitoring has received more and more attention. Zhou and Xue [1] summarized the monitoring methods and monitoring algorithms in the milling process, and Prashant Waydande and Chinchanikar [2] reviewed the monitoring system of tool wear. Generally speaking, the condition monitoring methods and systems of tool could be divided into two parts: one is physics-driven models, and the other is data-driven models. Physics-driven models explore a physical understanding of the tool in order to estimate the running state and wear degree. For example, Yen et al. [3] used Taylor's formula to estimate the tool wear. Zhu and Zhang [4] developed a generic explicit model with adjustable coefficients for flank wear of tool and then established a relationship between milling force and flank wear of tool. Therefore, it could use the tool wear model to predict the life. For example, Nouri et al. [5] proposed a method to monitor end milling tool wear in real-time by tracking the force model coefficient during the cutting process to predict the life to tool. However, the major challenges of physics-driven models included the following [6]: sufficient knowledge of the failure mechanism of tool wear was lacked, and the values of some parameters in the formulations were difficultly obtained. In order to avoid the comprehensive or complicated physical models, data-driven models were chosen and developed in recent years. Data-driven models tried to model or simulate the tool wear process by using the actual running data, including force, vibration, acoustic emission, spindle motor and feed currents, and so on. For example, Shankar et al. [7] used sound pressure and machining force to train a neural network to predict flank wear of tool during the milling process. Kalvoda and Hwang [8] used the Hilbert–Huang transform to process the acceleration vibration signal, and the results showed that the changing of frequency of the marginal spectra could reflect the geometric changing of the cutter tool. After carefully analyzing the acoustic emission signal by using statistical analysis, spectrum analysis, and wavelet packet, Leng et al. [9] proposed a method to detect the tool wear for drilling

the composite material. Sun et al. [10] studied the relationship between inverter input current and tool wear condition based on current virtual values which were calculated from the line current on the inverter input side. Proteau et al. [11] proposed a specific cutting energy, which used selected multifeatures to train a recurrent neural network, to predict the tool wear. In general, the data-driven models used machine learning algorithms or artificial intelligence algorithms to train a model, and then, the model could automatically recognize the complex patterns. But, the modeling process needed a large amount of historical data [12], especially failure data or degraded data, whereas the failure data or degraded data were very difficult to get. If we can only use one-class data to train a model, the modeling process would become much easier. Therefore, the concept of anomaly detection could help us.

Anomaly detection refers to the process of finding patterns in data that do not conform to expected behavior [13]. The nonconforming patterns include anomalies, outliers, discordant observations, exceptions, aberrations, surprises, and contaminants. The anomaly detection usually used normal data to train models because the nonconforming patterns were unknown and unexpected. So, if we consider the state of tool wear as nonconforming patterns, we could use anomaly detection methods to detect the state of tool wear. The models of anomaly detection included the density model, reconstruction model, and boundary model [14]. For example, the Gaussian model was a density model. If the distribution of unknown data was different with the distribution of the model, the unknown data could be considered as outlier. But, the density model needed typical data from the true data distribution and needed a large amount of training data for high dimension data. The self-organizing map (SOM) was a reconstruction model. It tried to reconstruct a new model in the new space after mapping the original data into a high-dimension space. But, it needed to assume the clustering characteristics of the training data. For the boundary model, it tried to find an optimized boundary around the target data, and the typical models were the support vector data description (SVDD) [15] and the nearest neighbor model. Because the nearest neighbor model tried to directly embrace the entire target data based on the distance information, the model was easily understood and used. Therefore, we choose the nearest neighbor model to describe the running data of tool. Moreover, the redundant and irrelevant features could affect the accuracy of the nearest neighbor model. Therefore, the sensitive features should be selected firstly. The rough set theory [16] could be used to select sensitive features based on the concept of lower approximation, upper approximation, and boundary region. Unfortunately, the rough set only processed discrete features, and continuous features should be discretized. But, the discretization could cause the loss of information. Then, Hu et al. [17] proposed the neighborhood rough set model. The neighborhood rough set can directly process continuous features based on the concept of neighborhood relationship. Therefore, we choose the neighborhood rough set model to select the sensitive features.

In order to monitor the wear condition of tool in process, a new assessment method based on the neighborhood rough set model and the nearest neighbor model is proposed. After selecting sensitive features by using the neighborhood rough set model, the wear condition of tool could be described by using the boundary curves which are trained from the nearest neighbor model. Finally, the quantitative assessment indicator is designed based on the areas which are created by the boundary curves in the two-dimension spaces.

2. Neighborhood Rough Set Model and Nearest Neighbor Model

One key definition of the neighborhood rough set model is the dependency degree. For example, the dependency degree of D to B is defined as the ratio of consistent objects:

$$r_B(D) = \frac{\left|\mathrm{POS}_B(D)\right|}{|U|}, \tag{1}$$

where U is the sample space. $\mathrm{POS}_B(D)$ calls the positive region. The positive region is the sample set which can be classified into one of the classes without uncertainty. $r_B(D)$ reflects the capability of B to approximate D.

Another key definition is the significance of a feature:

$$\mathrm{SIG}(a, B, D) = r_B(D) - r_{B-a}(D), \tag{2}$$

and if $\mathrm{SIG}(a, B, D) = 0$, feature a is superfluous in B; otherwise, a is indispensable.

Based on the concept of the neighborhood rough set model, the dependency would decrease if any sensitive feature is missed, and then, we could use the significance of a feature to evaluate each feature. At the beginning, the pool of selected features is empty. Then, we could traverse all features, finding the sensitive features which could make the SIG get maximum values and $\mathrm{SIG} > 0$. Finally, the sensitive features were added to the pool of selected features. The detailed description of feature selection algorithm could be found in [17].

The nearest neighbor model is a one-class classifier. It tries to estimate an hypersphere, which is centered around the test object $\mathbf{z}$, in d dimensions. The volume of the hypersphere is grown until it captures k objects from the training set. The local density could be estimated as follows:

$$p_{\mathrm{NN}}(z) = \frac{(k/N)}{V_k\left(\left\|z - \mathrm{NN}_k^{\mathrm{train}}(z)\right\|\right)}, \tag{3}$$

where $\mathrm{NN}_k^{\mathrm{train}}(\mathbf{z})$ is the k nearest neighbor of $\mathbf{z}$ in the training set and V_k is the volume of the hypersphere containing this object.

For the one-class classifier, a test object $\mathbf{z}$ is accepted when its local density is larger or equal to the local density of the first nearest neighbor in the training set $\mathrm{NN}^{\mathrm{train}}(\mathbf{z}) = \mathrm{NN}_1^{\mathrm{train}}(\mathbf{z})$.

3. Assessment Approach

It is very important how to quantitatively assess the degree of tool wear. Therefore, this section would focus on the quantitative indicator firstly. Pan et al. [18] proposed a quantitative assessment indicator based on the SVDD. After training a hypersphere of baseline state by using SVDD with the data of baseline state, the formulation of the center of the hypersphere of baseline state could be obtained. Then, the distance of the data of unknown state from the center of the hypersphere of baseline state could be calculated, and the value of distance could be considered as the quantitative assessment indicator. Although the SVDD and the nearest neighbor model all belong to the boundary model, there is no formulation of the center of the nearest neighbor model. So, it is difficult to calculate the distance. Besides, the distance cannot distinguish two different running states which have the same distance.

After getting the boundary curves of the baseline state and the unknown state by using the nearest neighbor model, the spatial position of two boundary curves could help us to determine the running condition. As shown in Figure 1(a), the intersection area could associate with the degree of similarity for two boundary models. The bigger the intersection area, the greater the similarity for two boundary models. As shown in Figure 1(b), the expanding area could associate with the degree of nonsimilarity for two boundary models. The bigger the expanding area, the greater the nonsimilarity for two boundary models. Therefore, the value of area could be considered as a quantitative indicator to assess the running condition. Moreover, the intersection area or expanding area can consider the effect of distance and angle simultaneously. The formulation of QAI is

$$\mathrm{QAI}_i = \begin{cases} \mathrm{Area}_{\mathrm{baseline}} + \mathrm{Area}_{i\text{th state}} - \mathrm{Area}_{\mathrm{intersection}} \text{ for intersection situation,} \\ \mathrm{Area}_{\mathrm{baseline}} + \mathrm{Area}_{i\text{th state}} + \mathrm{Area}_{\mathrm{expanding}} \text{ for expanding situation.} \end{cases} \tag{4}$$

The area is estimated by using the Monte Carlo method, taking intersection area as an example, as shown in Figure 2. Firstly, a square is created, and then, the area of square could be easily estimated, as $\mathrm{Area}_{\mathrm{square}}$. Secondly, uniformly scattering points over the square, the number of points is N_{total}. Thirdly, counting the number of points inside the square, the number is N_{inside}. Finally, the ratio of the intersection area and square area is equal to the ratio of the inside count and the total sample count, so the intersection area is $\mathrm{Area}_{\mathrm{intersection}} = (N_{\mathrm{inside}}/N_{\mathrm{total}})\mathrm{Area}_{\mathrm{square}}$.

The assessment process is shown in Figure 3. Firstly, the Milling Dataset is analyzed by using the neighborhood rough set model, and then, two sensitive features are selected. Secondly, we suppose that the degree of tool wear is very small at beginning stage, especially for first-time use. Therefore, the first test is selected as baseline state. Then, the boundary curve of baseline state can be obtained by using the nearest neighbor model. Thirdly, for unknown state, using same two sensitive features to train the nearest neighbor model, the boundary curve of unknown state can be obtained. Finally, the QAI which corresponds to the unknown state can be calculated, and the value of QAI can quantitatively describe the degree of tool wear.

4. Experimental Dataset, Results, and Discussion

4.1. Milling Dataset. In order to evaluate whether the assessment method is effective, the Milling Dataset [19], which is developed and provided by the NASA AMES and UC Berkeley, is used. The dataset contains 16 cases in which the milling parameters were varied for each case. In this paper, Case 1 and Case 5 are selected to research, and the experimental conditions of Case 1 and Case 5 are shown in Table 1.

Three different types of sensors, which include the acoustic emission sensor (WD925, PHYSICAL ACOUSTIC GROUP), vibration sensor(7201-50, ENDEVCO), and current sensor(OMRON K3TB-A1015 and CTA 213), were acquired at several positions. An acoustic emission sensor and a vibration sensor are each mounted to the table and the spindle of the machining center. The signals from all sensors are amplified and filtered and then fed through two RMS before they enter the computer for data acquisition. The signal from a spindle motor current sensor is fed into the computer without further processing. A 70 mm face mill with 6 inserts was chosen as the tool. The type of inserts is KC710 which is coated with multiple layers of titanium carbide, titanium carbonitride, and titanium nitride in sequence. Generally, the flank wear VB is used for evaluating tool wear. In experiments, VB is measured as the distance from the cutting edge to the end of the abrasive wear on the flank face of the tool. After the insert was taken out of the tool, the wear was measured by using a microscope. But, VB was measured between runs at irregular intervals and was not always measured. The description of the dataset is shown in Table 2.

Taking first dataset of Case 1 as an example, the signals of AC, DC, vibration table, vibration spindle, AE table, and AE spindle are shown in Figure 4. It can be found that there are three phases in the signal, which include the starting phase, operating phase, and stopping phase. Because we only want to focus on the tool wear during the operation phase, the data of the starting phase and stopping phase should be removed firstly.

Now, there are six features. However, the proposed new assessment indictor QAI only can be calculated in two-

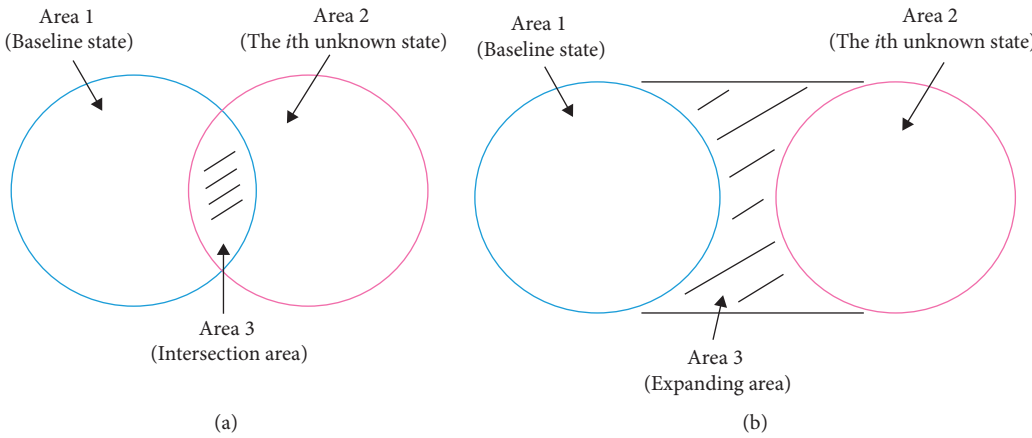

Figure 1: Schematic diagram of the assessment indicator. (a) Intersection situation. (b) Expanding situation.

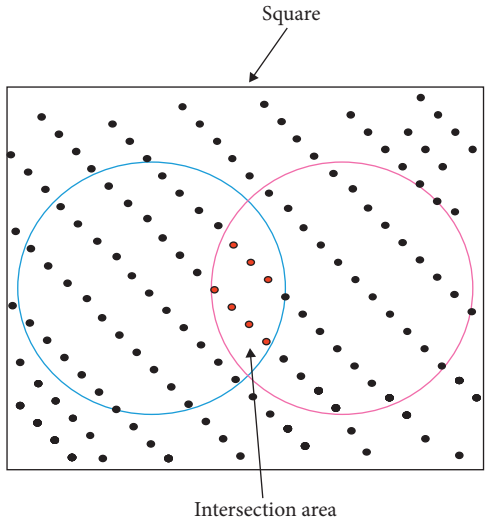

Figure 2: Schematic diagram of estimating the intersection area by using the Monte Carlo Method.

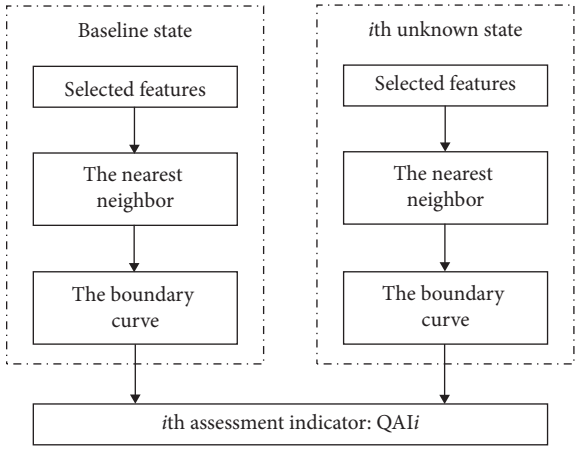

Figure 3: Flow chart of the assessment process.

dimension space. Therefore, two sensitive features should be selected secondly. AE spindle and vibration spindle as the sensitive features are selected by using the neighborhood rough set model. Taking the first dataset and seventh dataset of Case 1 as an example, multiboundary models are trained by using the nearest neighbor model with different pair of features, respectively, as shown in Figures 5 and 6. Comparing Figure 5(a) with Figure 6(a), it can be found that the value range of AE spindle and vibration spindle increases with time, implying that AE spindle and vibration spindle could more accurately reflect the state of tool wear. Comparing Figure 5(b) with Figure 6(b), it can be found that the value range of AE table and vibration table barely increases with time. Besides, the dispersion degree of the boundary model which uses AE table and vibration table is greater than that of the boundary model which uses AE spindle and vibration spindle. Moreover, it can be found that the distortion phenomenon for DC is as shown in Figure 6(c).

Table 1: Experimental conditions of Case 1 and Case 5 of the Milling Dataset.

Case	Depth of cut (mm)	Feed (mm/rev)	Material
1	1.5	0.5	Cast iron
5	1.5	0.5	Stainless steel J45

Taking Case 1 and Case 5 as an example, we assess the tool wear in process by using the method which is proposed in Section 3. The parameters of the nearest neighbor model are shown in Table 3.

4.2. The Assessment Result of Case 1. We choose AE spindle and vibration spindle as sensitive features to train the boundary model, and then, two different boundary curves are compared to find the intersection area or expanding area. Partial results are shown in Figures 7–12. Based on the intersection area or expanding area, we could calculate the assessment indicator QAI, as shown in Figure 13. The VB which was measured in experiment is shown in Figure 14.

4.3. The Assessment Result of Case 5. We compare two different boundary curves to find the intersection area or expanding area, as shown in Figures 15–19. Based on the intersection area or expanding area, we could calculate the

Table 2: Description of the dataset.

Name	Description
VB	Flank wear, measured after runs. Measures were not taken after each test
AC	AC spindle motor current
DC	DC spindle motor current
Vibration table	RMS of vibration at table
Vibration spindle	RMS of vibration at spindle
AE table	RMS of acoustic emission at table
AE spindle	RMS of acoustic emission at spindle

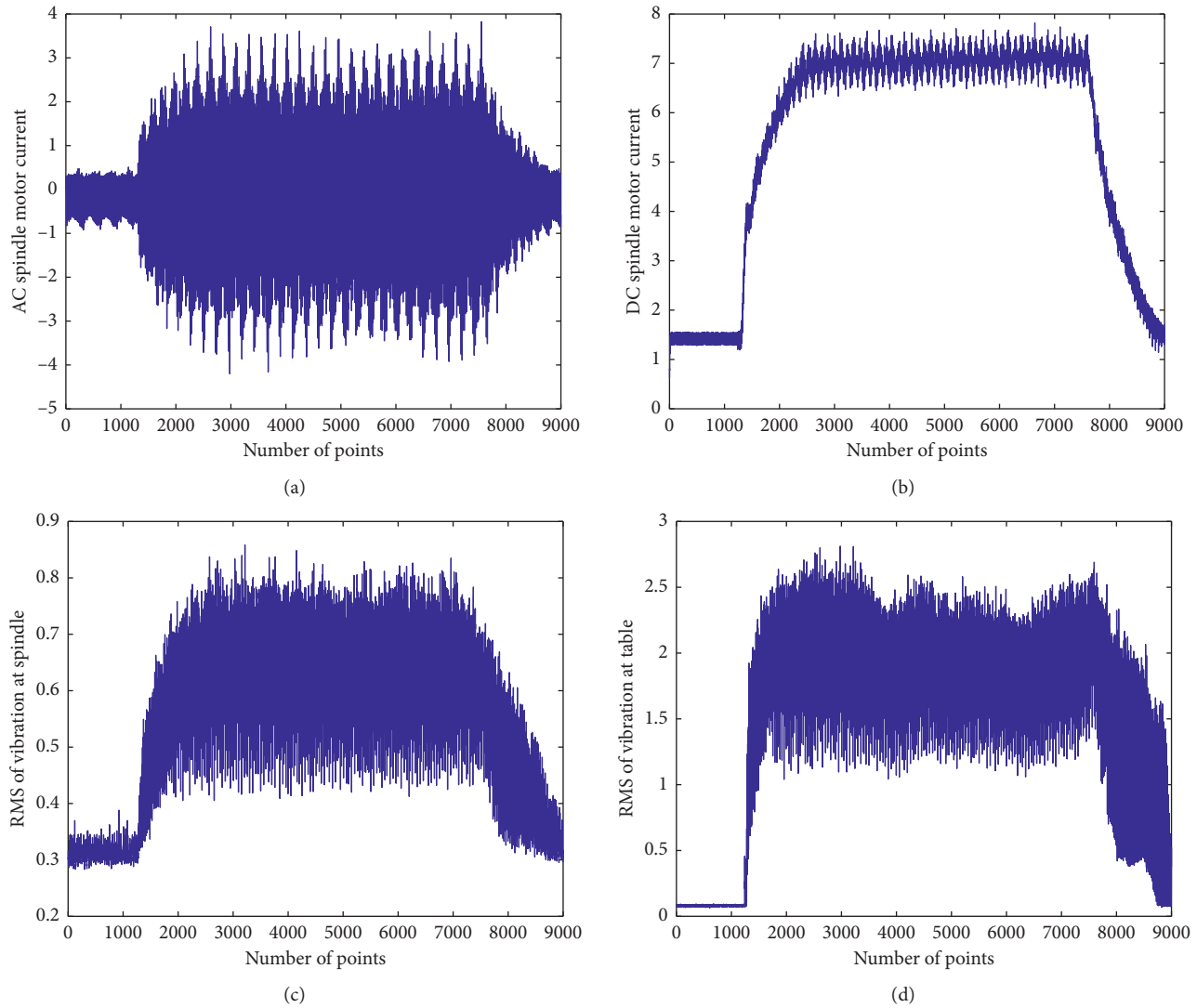

Figure 4: Continued.

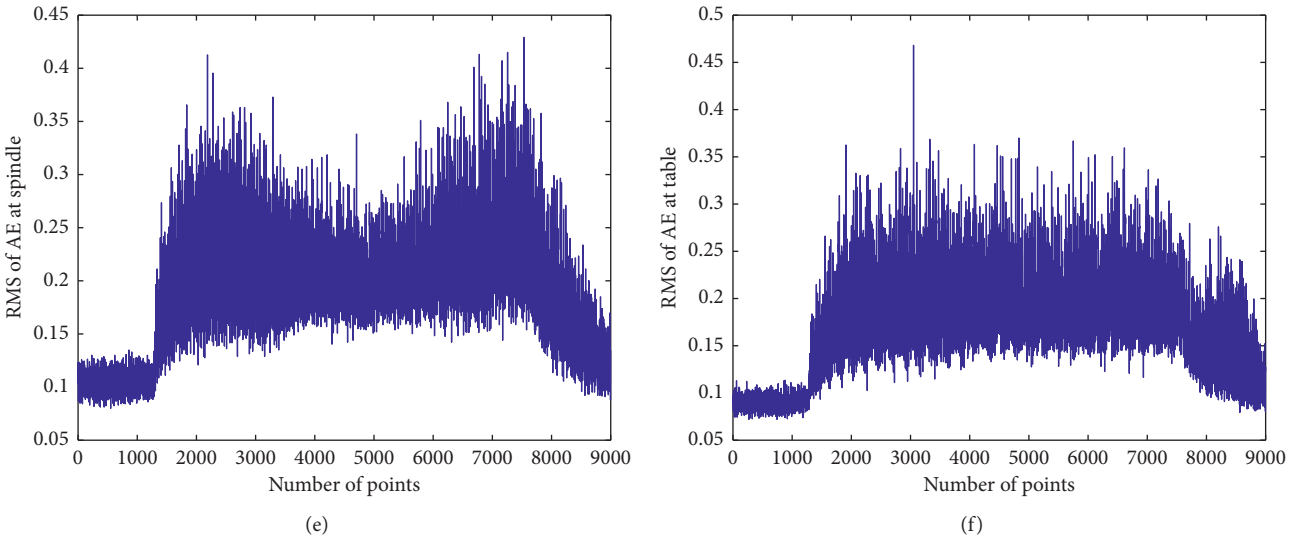

Figure 4: First dataset of Case 1 of the Milling Dataset. (a) AC spindle motor current. (b) DC spindle motor current. (c) RMS of vibration at spindle. (d) RMS of vibration at table. (e) RMS of AE at spindle. (f) RMS of AE at table.

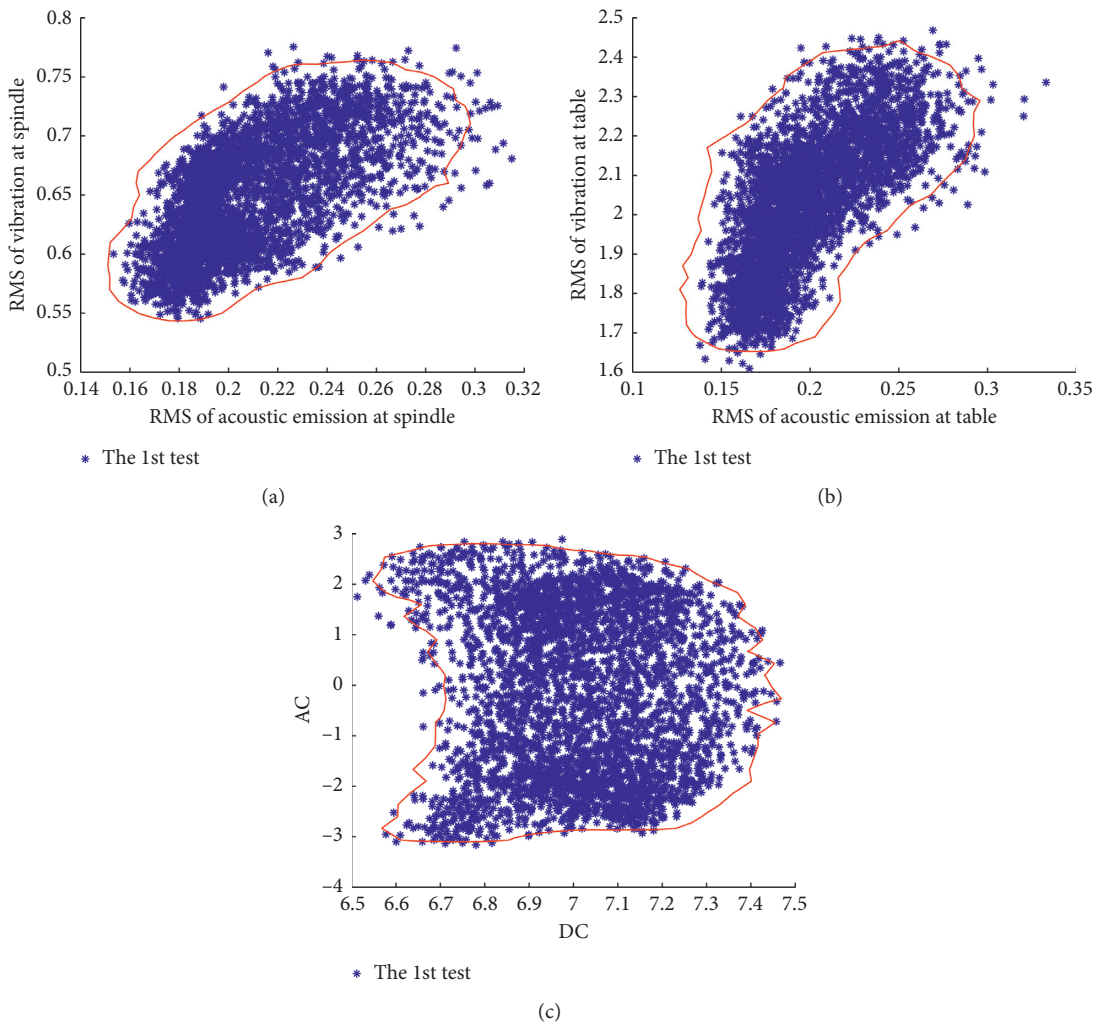

Figure 5: Different boundary curves of the first dataset of Case 1. (a) Features of the boundary curve are AE spindle and vibration spindle. (b) Features of the boundary curve are AE table and vibration table. (c) Features of the boundary curve are DC and AC.

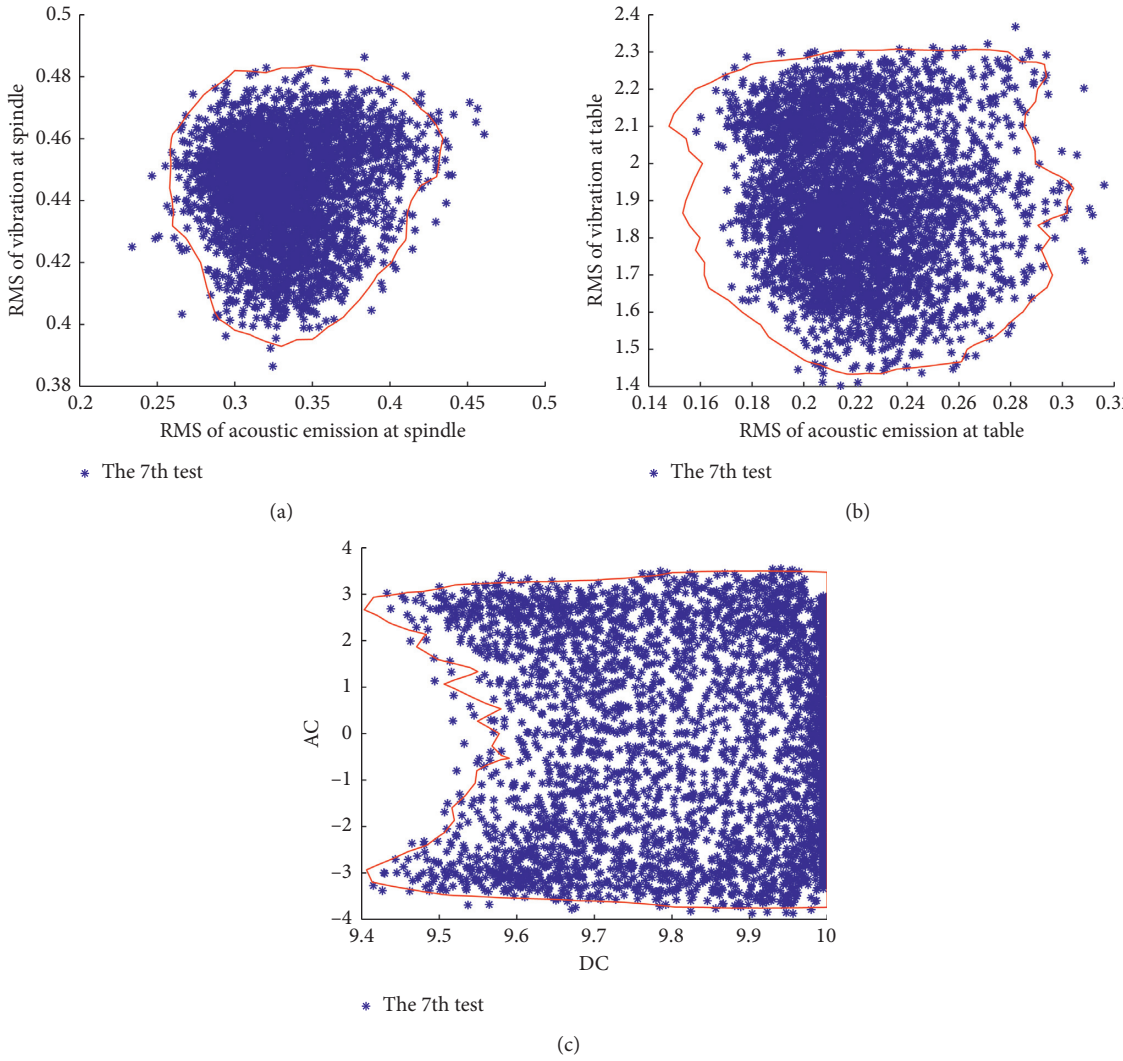

Figure 6: Different boundary curves of the seventh dataset of Case 1. (a) Features of the boundary curve are AE spindle and vibration spindle. (b) Features of the boundary curve are AE table and vibration table. (c) Features of the boundary curve are DC and AC.

Table 3: The parameters of the nearest neighbor model.

Features	The number of training samples	k nearest neighbor	Distance
AE spindle vibration spindle	3500	15	Euclidean distance

assessment indicator QAI, as shown in Figure 20. The VB which was measured in experiment is shown in Figure 21.

5. Discussion

In order to evaluate the degree of tool wear quantitatively, two new assessment indicators QAI are calculated for Case 1 and Case 2, as shown in Figures 13 and 20. Comparing with the corresponding VB which are shown in Figures 14 and 21, it can be found that the trend of QAI is basically consistent with VB.

For Case 1, the wear condition of tool could be divided into three parts. At the beginning stage which is from the 1st test to 6th test, the abrasion wear occurred because the insert should remove large chunks, and the wear of tool is very serious. The second stage is from the 7th test to 15th test; although the wear of tool is still increasing, the degree of wear slows down because the tool is in stable running condition. The third stage is from the 16th test to 17th test, and the tool is in accelerated wear condition.

No matter Case 1 or Case 5, it can be found that the test models gradually go away from the baseline mode with the increase in time. The intersection areas gradually decrease, and then, the expanding areas gradually increase. Moreover, except the changing about distance, the angle between the baseline model and test model is changing too. The angle informant is implicit in the

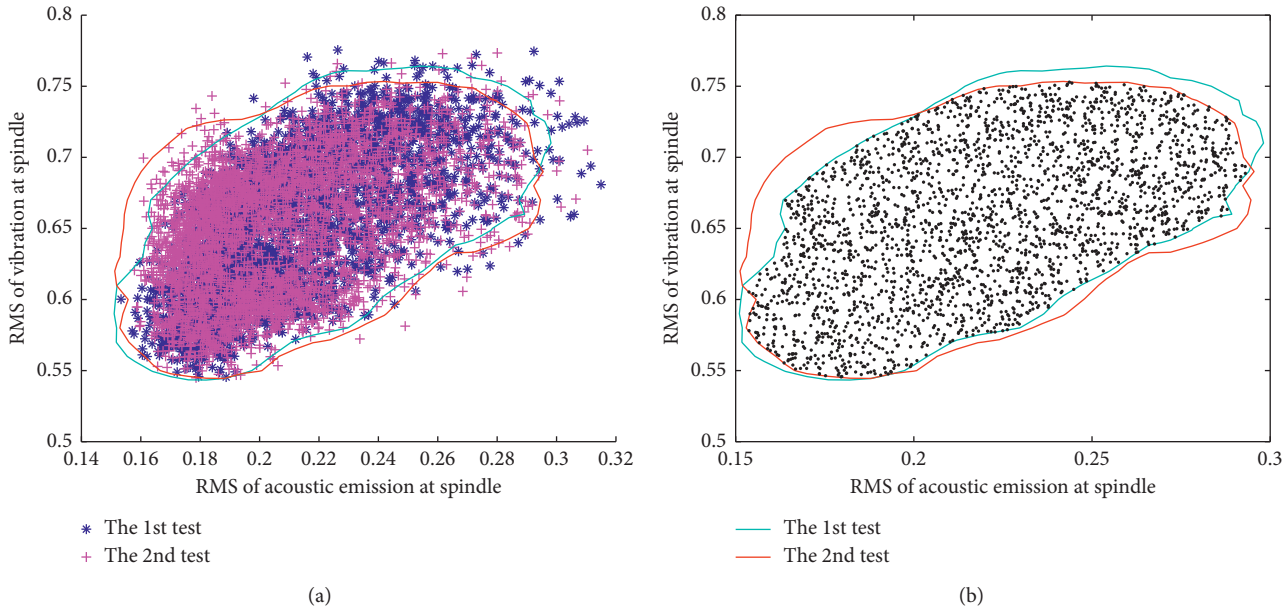

Figure 7: The 1st test vs. 2nd test for Case 1. (a) Two boundary models. (b) The intersection area.

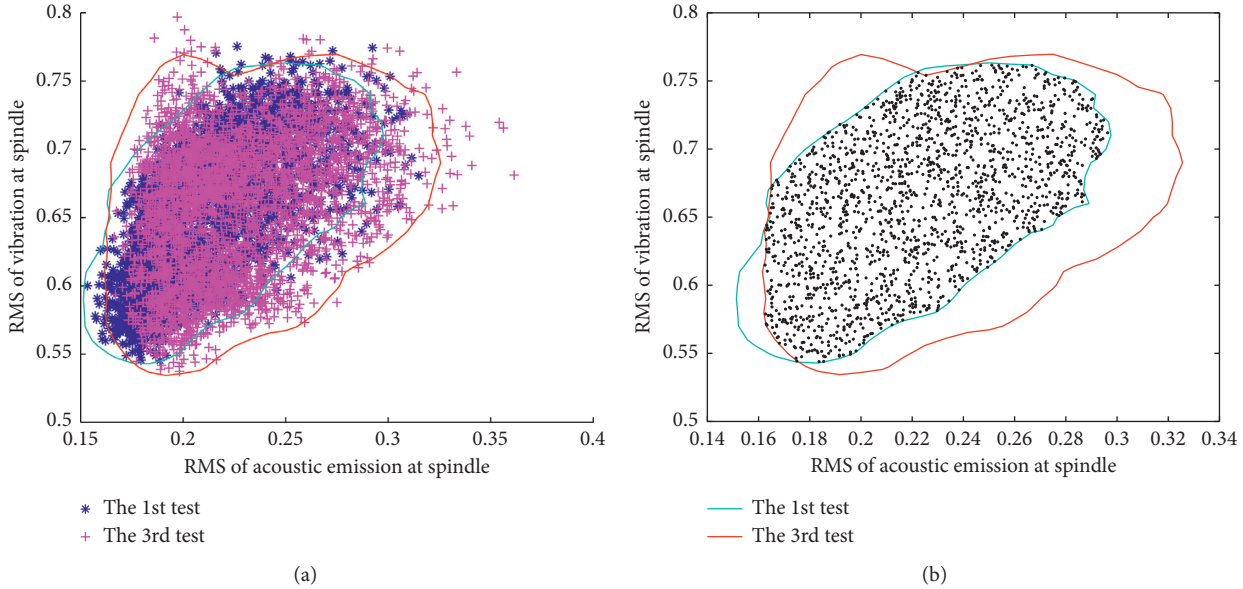

Figure 8: The 1st test vs. 3rd test for Case 1. (a) Two boundary models. (b) The intersection area.

intersection area or expanding area. For example, the comparing boundary curve of the 6th test with the boundary curve of the 5th test for Case 5 in Figures 18 and 19, it could be found that the boundary curve of the 6th test only expands in the X-direction because only the value of RMS of AE spindle changed significantly, whereas the value of RMS of vibration spindle almost remained constant. This phenomenon could be considered that the angles between two boundary curves are different. Mapping the angles into the expanding areas, the two expanding areas are different. Therefore, the intersection area or expanding area can reflect the effect of distance and angle simultaneously.

In order to evaluate the effect of different features, two new QAIs are calculated, as shown in Figures 22 and 23. One is using AE table and vibration table as features, and the other is using AC and DC as features. Comparing with Figure 20, it could be found that the trend of two QAIs is not good; especially as shown in Figure 22, the predicted degree of tool wear is not true.

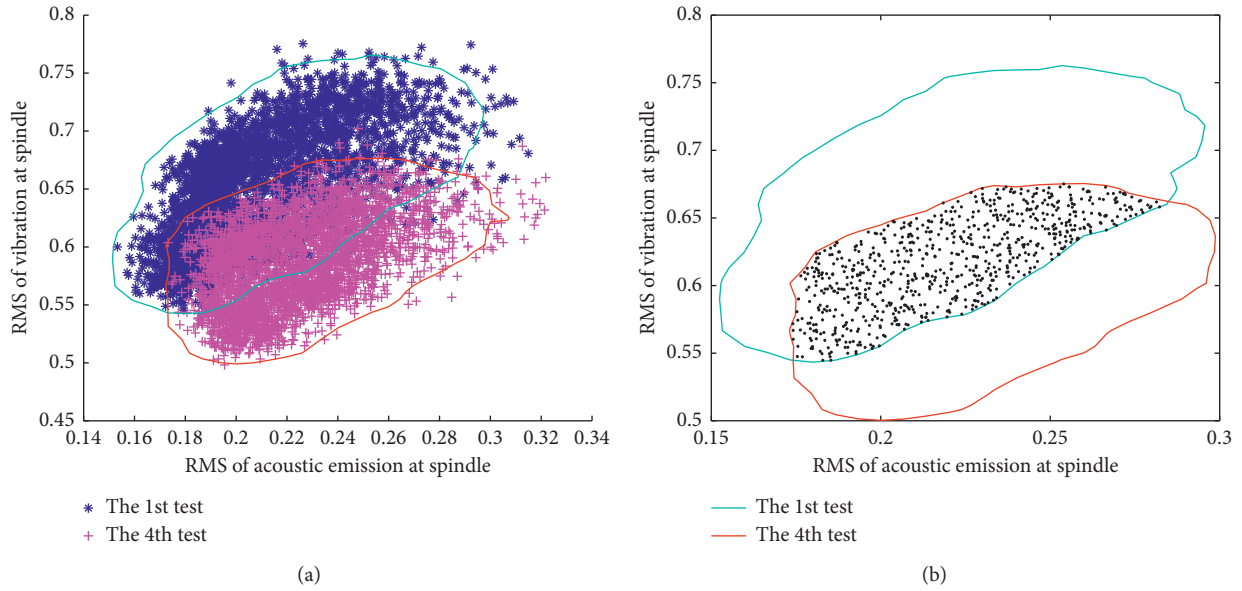

Figure 9: The 1st test vs. 4th test for Case 1. (a) Two boundary models. (b) The intersection area.

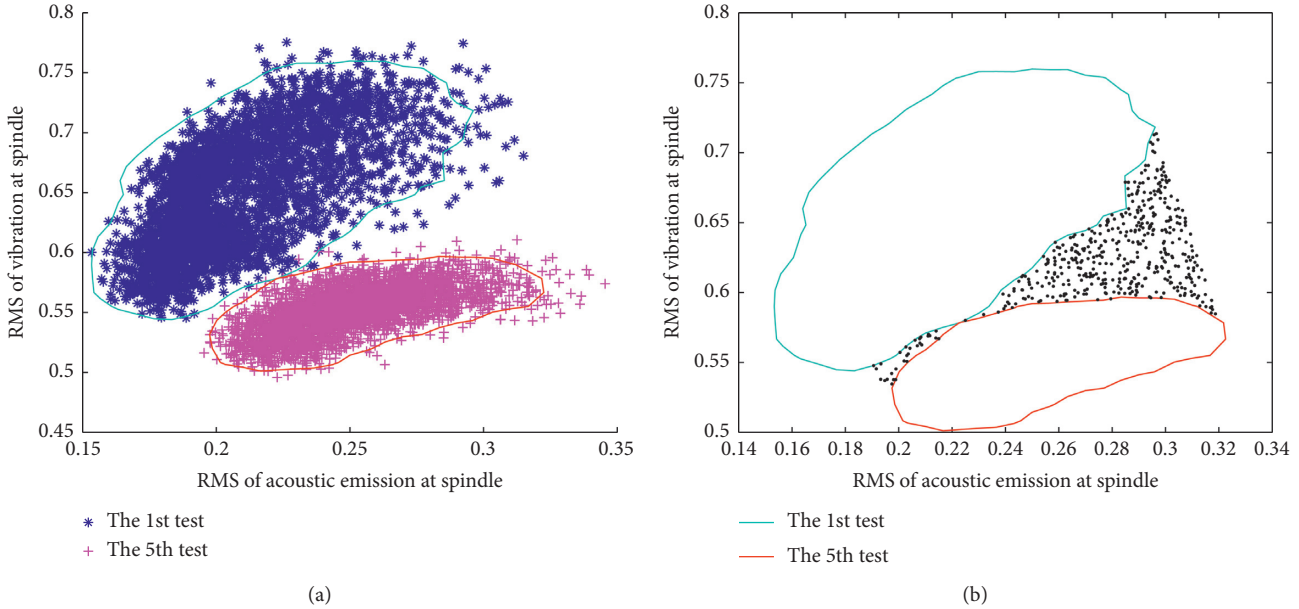

Figure 10: The 1st test vs. 5th test for Case 1. (a) Two boundary models. (b) The expanding area.

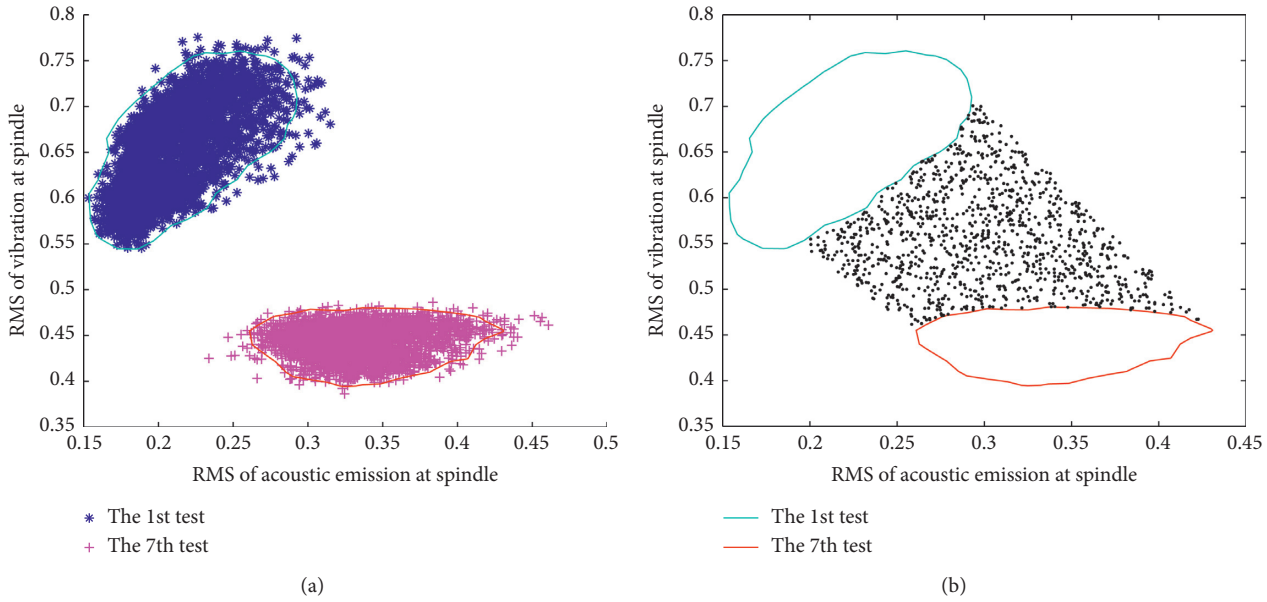

Figure 11: The 1st test vs. 7th test for Case 1. (a) Two boundary models. (b) The expanding area.

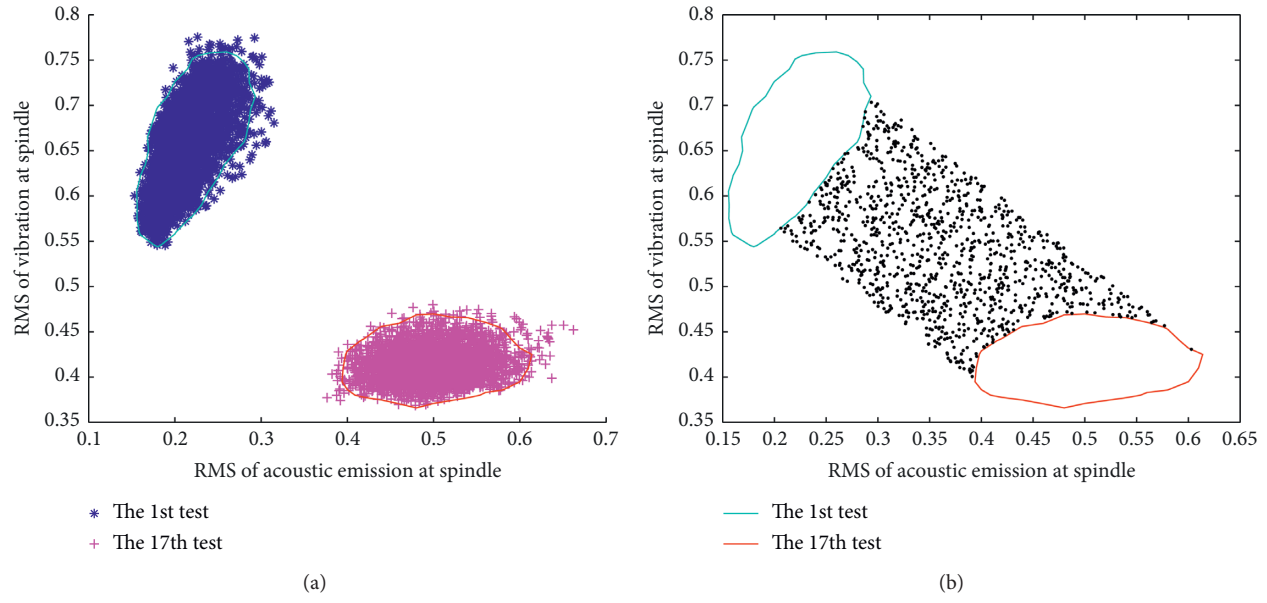

Figure 12: The 1st test vs. 17th test for Case 1. (a) Two boundary models. (b) The expanding area.

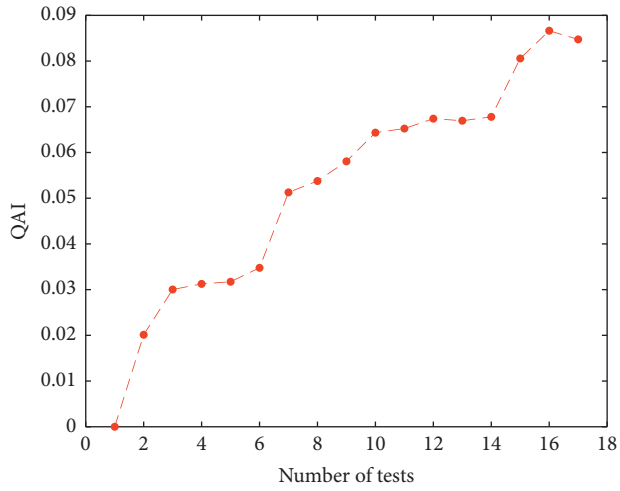

Figure 13: The QAI changing with the number of test for Case 1 (features are AE spindle and vibration spindle).

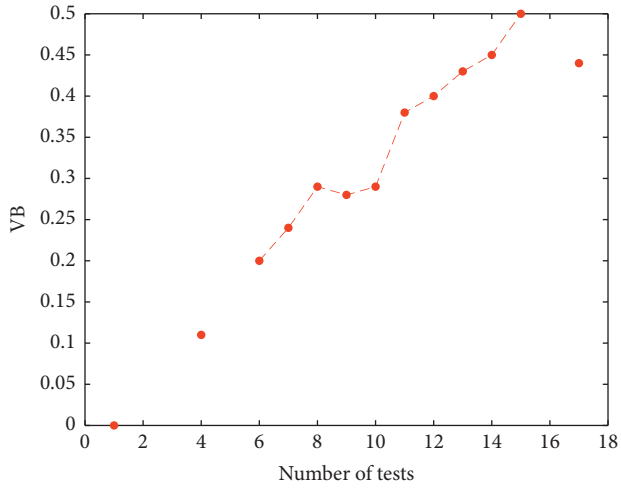

Figure 14: The VB changing with the number of test (missing values of 2nd, 3rd, 5th, and 16th test) for Case 1.

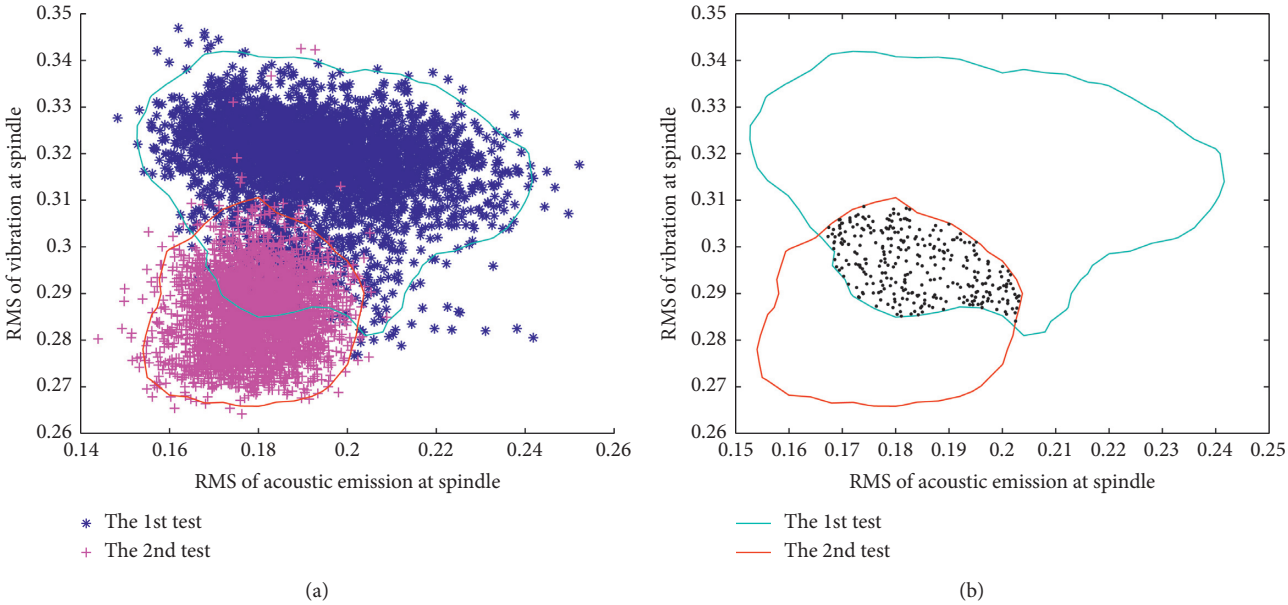

Figure 15: The 1st test vs. 2nd test for Case 5. (a) Two boundary models. (b) The intersection area.

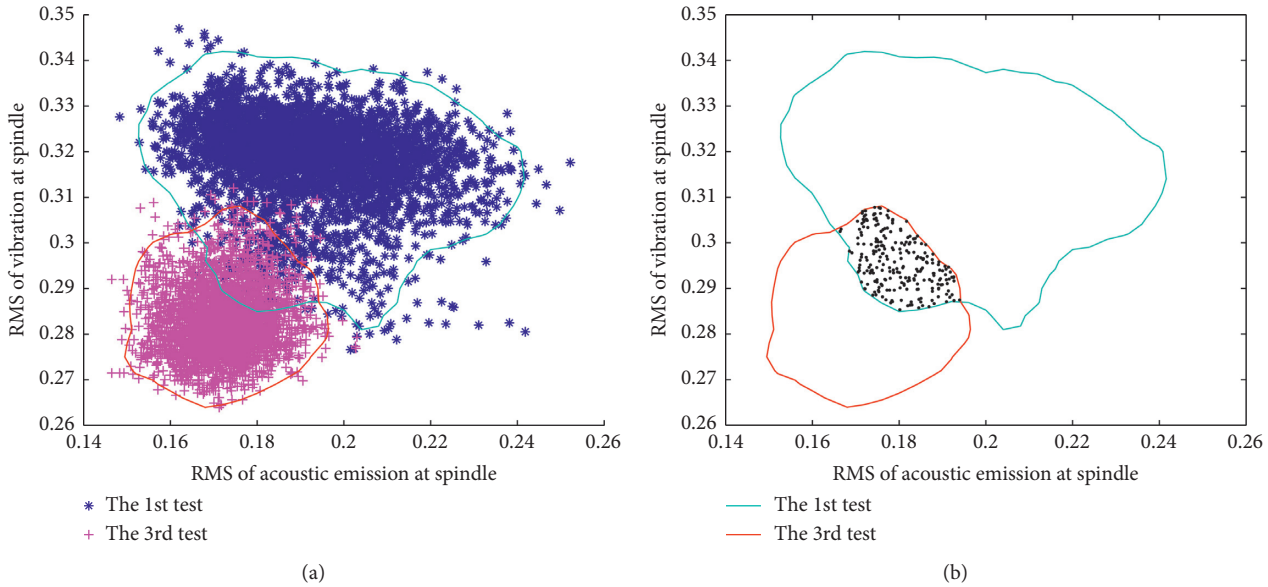

Figure 16: The 1st test vs. 3rd test for Case 5. (a) Two boundary models. (b) The intersection area.

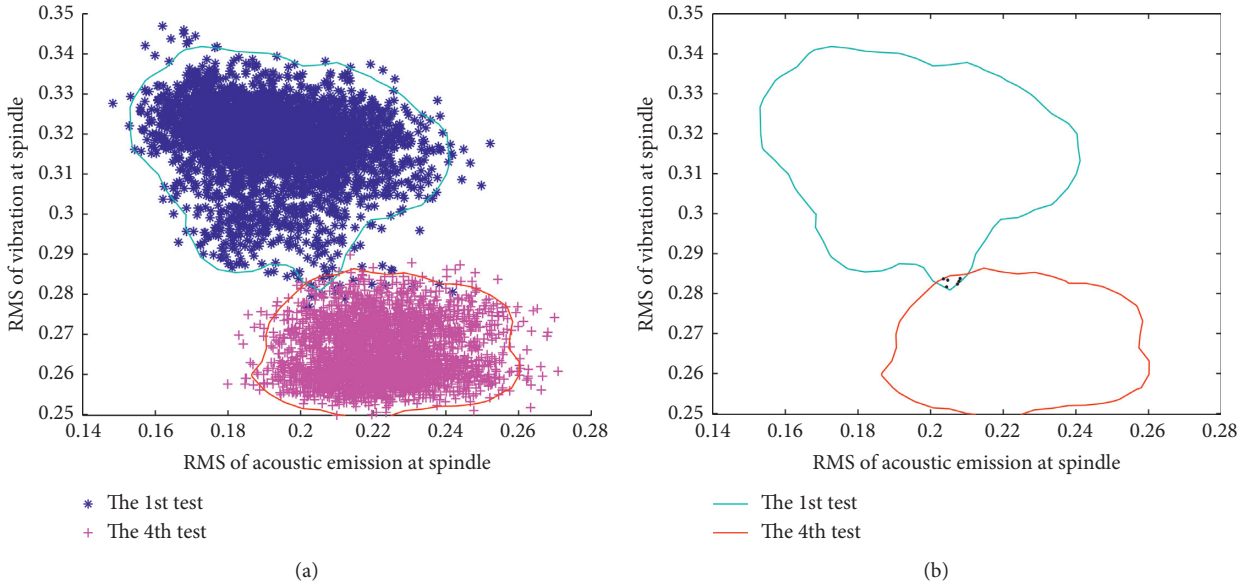

Figure 17: The 1st test vs. 4th test for case 5. (a) Two boundary models. (b) The intersection area.

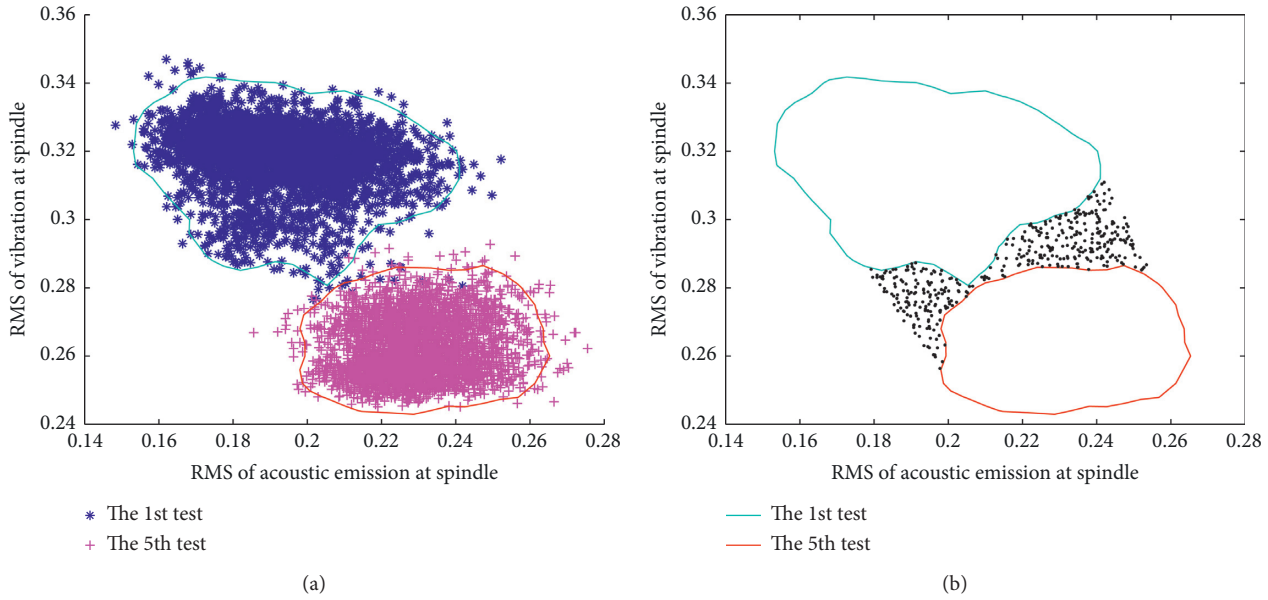

Figure 18: The 1st test vs. 5th test for Case 5. (a) Two boundary models. (b) The expanding area.

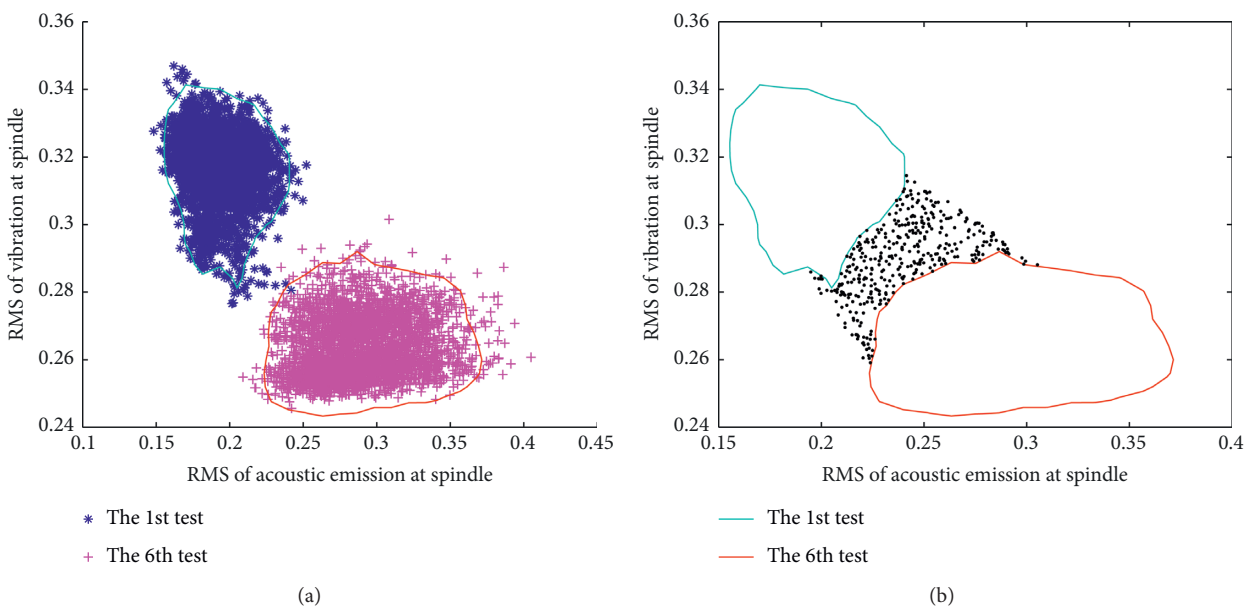

Figure 19: The 1st test vs. 6th test for Case 5. (a) Two boundary models. (b) The expanding area.

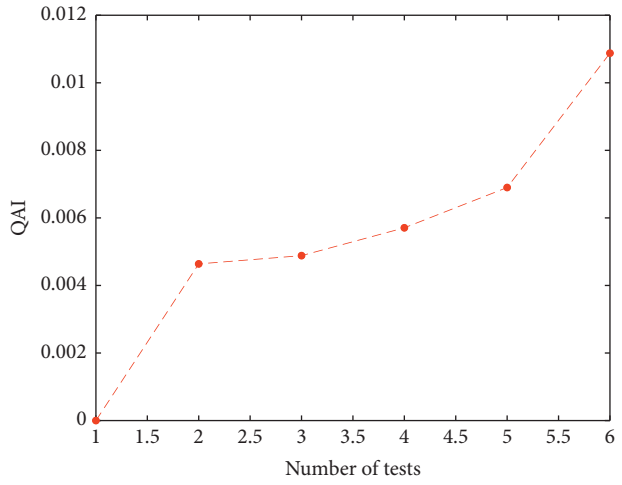

Figure 20: The QAI changing with the number of test for Case 5 (features are AE spindle and vibration spindle).

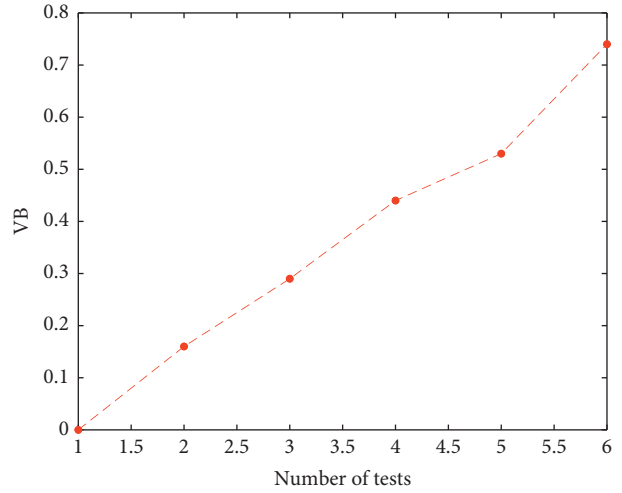

Figure 21: The VB changing with the number of test for Case 5.

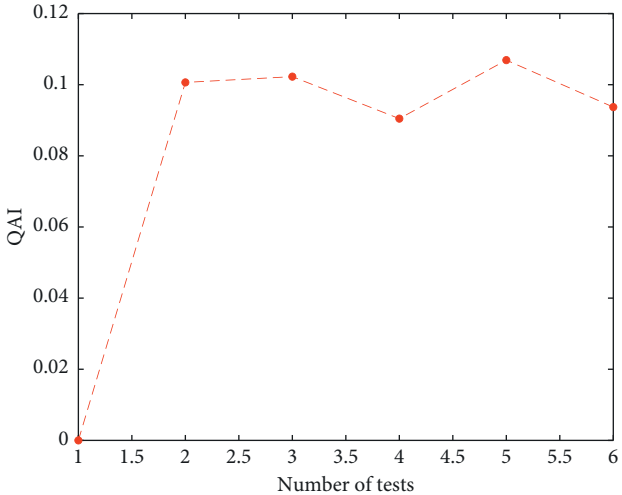

Figure 22: The QAI changing with the number of test for Case 5 (features are AE table and vibration table).

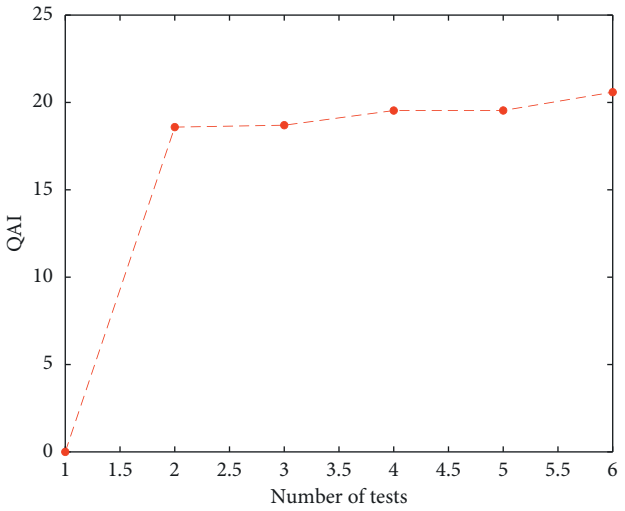

Figure 23: The QAI changing with the number of test for Case 5 (features are AC and DC).

6. Conclusions

After selecting two sensitive features by using the neighborhood rough set model, the boundary curves can be obtained based on the nearest neighbor model. And then, a new assessment process and a quantitative assessment indicator QAI are proposed. The main conclusions includethe following: (1) The boundary curve, which is trained based on selected features, can clearly describe the running state in two-dimension spaces. (2) The intersection area or expanding area can comprehensively consider the effect of distance and angle between the baseline curve and unknown curve. (3) The QAI can quantitatively describe the degree of wear of tool. (4) Unlike with the traditional indicator VB which only is measured offline when we disassemble the inserts from the tool, it is easy to monitor the tool wear in process using the QAI.

Data Availability

The previously reported Milling Dataset was used to support this study and is available at the NASA Ames Prognostics Data Repository. The prior studies (and datasets) are cited at relevant places within the text as references: A. Agogino and K. Goebel (2007), BEST lab, UC Berkeley. "Milling Dataset," NASA Ames Prognostics Data Repository (http://ti.arc.nasa.gov/tech/dash/groups/pcoe/prognostic-data-repository/), NASA Ames Research Center, Moffett Field, CA.

Conflicts of Interest

The authors declare that there are no conflicts of interest regarding the publication of this paper.

Acknowledgments

The authors thank UC Berkeley and the NASA Ames Prognostic Data Repository for providing the Milling Dataset.

References

[1] Y. Zhou and W. Xue, "Review of tool condition monitoring methods in milling processes," *The International Journal of Advanced Manufacturing Technology*, vol. 96, no. 5–8, pp. 2509–2523, 2018.

[2] N. A. Prashant Waydande and S. Chinchanikar, "A review on tool wear monitoring system," *Journal of Mechanical Engineering and Automation*, vol. 6, no. 5A, pp. 49–53, 2016.

[3] Y.-C. Yen, J. Söhner, B. Lilly, and T. Altan, "Estimation of tool wear in orthogonal cutting using the finite element analysis," *Journal of Materials Processing Technology*, vol. 146, no. 1, pp. 82–91, 2004.

[4] K. Zhu and Y. Zhang, "A generic tool wear model and its application to force modeling and wear monitoring in high speed milling," *Mechanical Systems and Signal Processing*, vol. 115, pp. 147–161, 2019.

[5] M. Nouri, B. K. Fussell, B. L. Ziniti, and E. Linder, "Real-time tool wear monitoring in milling using a cutting condition independent method," *International Journal of Machine Tools and Manufacture*, vol. 89, p. 1, 2015.

[6] Ö. Eker, F. Camci, and I. K. Jennions, "Major challenges in prognostics: study on benchmarking prognostics datasets," in *Proceedings of the 1st European Conference of the Prognostics and Health Management Society*, pp. 148–145, Nantes, France, July 2012.

[7] S. Shankar, T. Mohanraj, and R. Rajasekar, "Prediction of cutting tool wear during milling process using artificial intelligence techniques," *International Journal of Computer Integrated Manufacturing*, vol. 32, no. 2, pp. 174–182, 2018.

[8] T. Kalvoda and Y.-R. Hwang, "A cutter tool monitoring in machining process using Hilbert-Huang transform," *International Journal of Machine Tools and Manufacture*, vol. 50, no. 5, pp. 495–501, 2010.

[9] S. Leng, Z. Wang, T. Min, Z. Dai, and G. Chen, "Detection of tool wear in drilling CFRP/TC4 stacks by acoustic emission," *Journal of Vibration Engineering & Technologies*, vol. 8, no. 3, pp. 463–470, 2019.

[10] W. Sun, M. Huang, Y. He, and K. Li, "Design of tool-state monitoring system based on current method," *The Journal of Engineering*, vol. 2019, no. 23, pp. 9026–9030, 2019.

[11] A. Proteau, A. Tahan, and M. Thomas, "Specific cutting energy: a physical measurement for representing tool wear," *The International Journal of Advanced Manufacturing Technology*, vol. 103, no. 1–4, pp. 101–110, 2019.

[12] X. Jin, Z. Que, Y. Sun, Y. Guo, and W. Qiao, "A data-driven approach for bearing fault prognostics," *IEEE Transactions on Industry Applications*, vol. 55, no. 4, pp. 3394–3401, 2019.

[13] R. A. Ariyaluran Habeeb, F. Nasaruddin, A. Gani, I. A. Targio Hashem, E. Ahmed, and M. Imran, "Real-time big data processing for anomaly detection: a survey," *International Journal of Information Management*, vol. 45, pp. 289–307, 2019.

[14] D. Tax, *One-Class Classification; Concept-Learning in the Absence Of Counter-examples*, Technische Universiteit Delft, Delft, Netherlands, 2001.

[15] D. M. J. Tax and R. P. W. Duin, "Support vector data description," *Machine Learning*, vol. 54, no. 1, pp. 45–66, 2004.

[16] Z. Pawlak, "Rough set theory and its applications to data analysis," *Cybernetics and Systems*, vol. 29, no. 7, pp. 661–688, 1998.

[17] Q. Hu, D. Yu, and Z. Xie, "Neighborhood classifiers," *Expert Systems with Applications*, vol. 34, no. 2, pp. 866–876, 2008.

[18] Y. Pan, J. Chen, and X. Li, "Bearing performance degradation assessment based on lifting wavelet packet decomposition and fuzzy c-means," *Mechanical Systems and Signal Processing*, vol. 24, no. 2, pp. 559–566, 2010.

[19] A. Agogino and K. Goebel, *BEST Lab, UC Berkeley, "Milling Data Set," NASA Ames Prognostics Data Repository*, NASA Ames Research Center, Moffett Field, CA, USA, 2007.